Short-wavelength quantum cascade lasers

Dmitry G. Revin*[a], Shiyong Zhang[a], Matthew J. Steer[b], Robert J. Airey[b], Andrey B. Krysa[b], Mark Hopkinson[b], Luke R. Wilson[a], Stefan Menzel[a], John W. Cockburn[a]
[a]Department of Physics and Astronomy, University of Sheffield, Sheffield S3 7RH, United Kingdom
[b]EPSRC National Centre for III- V Technologies, University of Sheffield, Sheffield S1 3JD, United Kingdom

ABSTRACT

We report the first realization of short wavelength ($\lambda \sim 3.05 - 3.6$ μm) lattice matched $In_{0.53}Ga_{0.47}As/AlAs_{0.56}Sb_{0.44}/InP$ quantum cascade lasers (QCLs). The highest-performance device ($\lambda \sim 3.6$μm) displays pulsed laser action for temperatures up to 300 K. The shortest wavelength QCL ($\lambda \approx 3.05$ μm) operates in pulsed mode at temperatures only up to 110 K. The first feasibility study of the strain compensated InGaAs/AlAsSb/InP QCLs ($\lambda \sim 4.1$ μm) proves that the lasers with increased indium fractions in the InGaAs quantum wells of 60 and 70% display no degradation compared with the lattice matched devices having identical design. This strain compensated system, being of particular interest for QCLs at $\lambda <\sim 3.5$μm, provides increased energy separation between the Γ and X conduction band minima in the quantum wells, thus decreasing possible carrier leakage from the upper laser levels by intervalley scattering. We also demonstrate that the performance of strain compensated InGaAs/AlAsSb QCLs can be improved if AlAsSb barriers in the QCL active region are replaced by AlAs layers. The introduction of AlAs is intended to help suppress compositional fluctuations due to inter diffusion at the quantum well/barrier interfaces.

Keywords: Quantum cascade lasers, intersubband transitions, mid-infrared emission, short-wavelength operation, strain compensation

1. INTRODUCTION

Until very recently, most developments in the field of mid IR quantum cascade lasers (QCLs) have been achieved in the longer part ($\lambda > 5$ μm) of the wavelength range, and only in the last few years has any significant progress been made for "short wavelength" QCLs emitting in the very short wavelength limit of the $\lambda \approx 3$ - 5 μm atmospheric window. To accommodate the high energy intersubband transitions required for short wavelength operation, the devices must be based on materials systems with relatively large conduction band offsets (ΔE_c). As a result, laser operation at wavelengths near 3 μm has been achieved for QCLs based on systems such as strain compensated InGaAs/(In)AlAs/InP ($\Delta E_c > \sim 700$ meV), InAs/AlSb/InAs ($\Delta E_c \sim 2$ eV) and $In_{0.53}Ga_{0.47}As/AlAs_{0.56}Sb_{0.44}/InP$ ($\Delta E_c \sim 1.6$ eV). Near room temperature pulsed laser emission at wavelengths as short as 2.95 and 3.14 μm [1,2] and very high power room temperature pulsed emission at $\lambda \approx 3.3$ μm [3] have been reported for InAs/AlSb devices and low temperature pulsed laser operation at $\lambda \approx 3.05$ μm has been demonstrated for InP-based strain compensated $In_{0.73}Ga_{0.27}As/In_{0.55}Al_{0.45}As/AlAs$ QCLs.[4] Room temperature continuous wave emission has been presented for strain compensated InGaAs/AlInAs/InP QCLs at wavelengths as short as 3.8 μm.[5]

The InGaAs/AlAsSb on InP system is of particular interest for short wavelength QCL development, since it combines a very high ΔE_c with compatibility with well-established InP device processing and waveguide technology. However until recently QC laser action has been observed in this materials system for wavelengths only above 3.7 μm ($\lambda \approx 3.9$ μm at room temperature).[6] Moreover, it has been suggested [2,6] that QCL operation may not be possible at wavelengths below about 3.7 μm in the devices based on $In_{0.53}Ga_{0.47}As$ quantum wells lattice matched to InP. The basis for this assertion is that for shorter wavelengths, the upper laser level (confined by the Γ-point conduction band profile) is calculated to lie higher in energy than the expected position of the X-point conduction band minima ($E(\Gamma\text{-}X) \approx 520$ meV for

* d.revin@sheffield.ac.uk; phone +44 114 222-3599; fax +44 114 222-3555

Novel In-Plane Semiconductor Lasers VII, edited by Alexey A. Belyanin, Peter M. Smowton,
Proc. of SPIE Vol. 6909, 69090V, (2008) · 0277-786X/08/$18 · doi: 10.1117/12.775316

$In_{0.53}Ga_{0.47}As$.[7] Such a situation might be expected to lead to a reduction in injection efficiency and/or intersubband population inversion due to intervalley scattering, and hence suppression of laser action.

Despite very encouraging recent results InGaAs/AlAsSb QCLs still show inferior performance at high temperatures compared with lattice matched and strain compensated Sb-free InGaAs/AlInAs lasers, even though the latter heterostructure system has much lower conduction band offset. One potential limitation in InGaAs/AlAsSb laser performance arises from the strong compositional fluctuations at quantum well/barrier interfaces due to inter diffusion and doping induced interface disorder.[8] It was shown previously in intersubband absorption experiments [9] that introduction of AlAs even one monolayer thick at the InGaAs/AlAsSb interfaces in multi quantum well structures results in significant reduction of the inter diffusion related effects. In the case of QCLs the quality of InGaAs/AlAsSb interfaces is a key issue because inter diffusion could lead to the uncontrolled modification of the conduction band profile (and electron effective masses) and increased broadening of the gain spectrum. The insertion of AlAs layers between InGaAs and AlAsSb should help to inhibit inter diffusion, thus improving the interface quality. Such improvement is more important in the active region parts of the cascade periods where the intersubband laser transitions occur and less influential in the injector regions.

In this report we explore the short wavelength limits for QCLs based on lattice matched $In_{0.53}Ga_{0.47}As/AlAs_{0.56}Sb_{0.44}/InP$ and show that the expected onset of Γ-X intervalley scattering does not stop laser action in lattice matched $In_{0.53}Ga_{0.47}As/AlAs_{0.56}Sb_{0.44}/InP$ QCLs at wavelengths below 3.7 μm. The lasers are demonstrated in which $\lambda \approx 3.6$ μm laser emission is observed at temperature of 300 K ($\lambda \approx 3.4$ μm at 80 K), with wavelengths as low as 3.05 μm being obtained from an alternative design at temperatures up to 110 K. We also report the development of strain compensated devices, in which the indium concentration in the quantum wells is increased from 53% up to 60 and 70%. In the latter structures, the Γ-X separation is increased by up to 100 meV and is expected to extend the short wavelength limit for laser transitions to be free from the effects of intervalley scattering. We also verify that strain compensated $In_{0.6}Ga_{0.4}As/AlAs_{0.67}Sb_{0.33}$ QCLs with AlAs barriers in the active region demonstrate much better performance compared with the lasers having identical design but with $AlAs_{0.67}Sb_{0.33}$ throughout the whole core region.

2. EXPERIMENTAL RESULTS

2.1 Design, waveguide and growth details

Six QCL structures (M3253, M3254, M3255, M3257, M3259 and M3260) were studied with core regions each comprising 30 periods of active and injector regions and based on a bound to continuum active region, [10] shown previously [11] to demonstrate better performance than devices with a three quantum well design. Specific details of individual device designs are given in the appropriate sections below. The design calculations were based on solving the Schrödinger equation using a one band model with an energy dependent effective mass in InGaAs layers.

The overall layer thicknesses starting at the high doped ($n \approx 10^{18}$ cm^{-3}) InP substrate are as follows: 2 μm low-doped (2×10^{17} cm^{-3}) InP/ 0.2 μm low-doped (2×10^{17} cm^{-3}) $In_{0.53}Ga_{0.47}As$ spacer/ core region/ 0.2 μm low-doped $In_{0.53}Ga_{0.47}As$ spacer / 2 μm low-doped InP/ 1 μm highly doped InP/ metal contact. The core regions and spacer layers were grown by molecular beam epitaxy (MBE) and InP cladding layers were deposited by metal organic vapour phase epitaxy.

Prior to the growth of QCL structures calibration growth was made on test superlattice structures with periods similar to those in the injectors of QCLs. The higher indium fraction in InGaAs layers for strain compensated lasers compared with lattice matched system was regulated by two separate indium sources. During these calibrations appropriate fractions of As and Sb in AlAsSb barriers were found for lattice matched and various strain compensated compositions in order to maintain minimal overall strain. A growth interruption of several seconds was employed at every InGaAs/AlAsSb interface while maintaining continuous As flux. The growth interruptions help to reduce compositional grading across these interfaces.

To assess structural quality, thickness and residual strain, all grown wafers were characterized by high resolution X-ray diffraction (XRD). XRD data obtained for a typical strain compensated test superlattice structure (100 periods of $In_{0.67}Ga_{0.33}As$ (2.2 nm) / $AlAs_{0.76}Sb_{0.24}As$ (1.3nm)) are shown in Fig.1. Very close positions of the zero-order peaks

originating from InP substrate and the superlattice as well as measured superlattice period of 3.6 nm, very similar to the intended value, indicate a high degree of growth control and balancing of the strain.

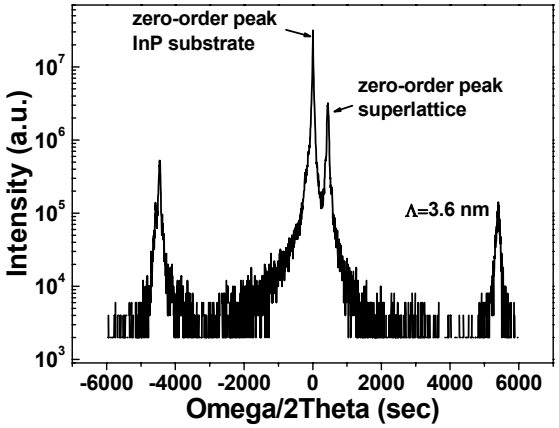

Fig. 1. X-ray diffraction for the strain compensated 100 period $In_{0.67}Ga_{0.33}As$ (2.2 nm) / $AlAs_{0.76}Sb_{0.24}As$ (1.3nm) superlattice structure grown on InP substrate.

Well resolved characteristic fringes due to the periodic QCL structure were also observed in a 10000 arcsec wide θ-2θ scan for each QCL sample indicating a good reproducibility of the layer thicknesses along the cascading periods. The QCL periods, as derived from the spacing between the fringes, were very similar within experimental error to the nominal values for all wafers.

The QCL wafers were processed by wet etching into laser ridge structures 20-30 μm wide and 1.5 mm long. Non-alloyed Ti/Au top and bottom contacts were used and the devices were soldered epilayer-up without facet coatings on copper submounts. The samples were mounted onto the cold finger of closed cycle helium cryostat and driven at 5 kHz with 50 ns pulses. Laser emission spectra were measured with a Fourier transform spectrometer and liquid nitrogen-cooled MCT detector using step scan and lock-in detection techniques. Light-current characteristics were obtained with a calibrated thermopile detector.

2.2 Lattice matched lasers

The calculated conduction band profiles under applied bias (including moduli squared of the relevant electron wave functions), are shown in Fig. 2 for lattice matched $In_{0.53}Ga_{0.47}As/AlAs_{0.56}Sb_{0.44}$/InP M3255 (λ = 3.5 μm) and M3253 (λ = 3.1 μm) lasers. The energy positions of the upper laser levels for these lasers are expected to be about 20 meV and 120 meV respectively above the position of the X-point ground state in the widest quantum wells of their active regions.

Both M3255 and M3253 devices display laser emission very close to the calculated wavelengths. The longer wavelength laser M3255 shows much better performance with threshold current density (J_{th}) of 2.6 kA/cm^2 at 80 K rising to about 10.5 kA/cm^2 at 300 K. The emission wavelength shifts from 3.42 μm at 80 K to 3.57 μm at 300 K. The characteristic temperature T_0 obtained by fitting the dependence of J_{th} versus temperature T in the range of 180 - 300 K using $J_{th} = J_0 \exp(T/T_0)$ is estimated to be about 130 K. The pulsed optical peak power for the M3255 laser is measured to be several hundreds of mW for most temperatures and is still about 30mW at 300 K. A steady increase of emission power is observed with increasing current, with no saturation or "roll-over" of the light-current curves. This is consistent with very good electron injection efficiency and alignment between the lowest electron levels in the injectors and the upper laser levels being maintained across a wide operating range.

The performance characteristics of the λ ~ 3 μm QCL (Fig. 3) are clearly inferior to those of M3255 device. The shorter wavelength laser M3253 emits only at temperatures below 110 K with J_{th} ~ 12 kA/cm^2 at 20 K and maximum optical peak power of about 20 mW. The device displays laser action over a relatively limited range of current with pronounced roll-over behaviour in the light-current characteristics. This possibly arises from inefficient electron injection into the upper laser levels and/or insufficient doping concentration in the injectors to sustain higher current. The voltage-current characteristic for this device shows a step-like voltage increase for current densities of about 16-17 kA/cm^2 consistent with the onset of misalignment between injector levels and upper laser level.

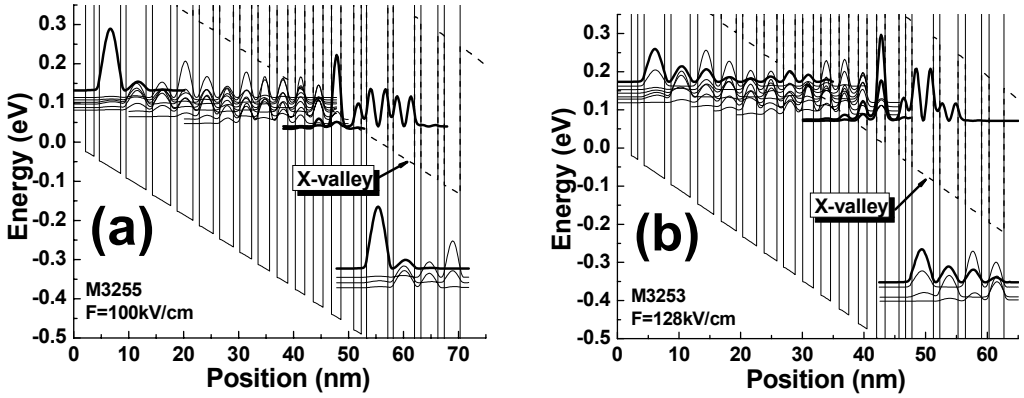

Fig. 2. Calculated conduction band profiles under applied bias for two active regions and one injector of lattice matched InGaAs/AlAsSb QCLs M3255 (a) and M3253 (b). The expected positions of the X-valley minimum are shown by dashed lines. The layer thicknesses (in nanometers) starting from the injection barrier for one period of active and injector regions are as follows: **2.3**/1.4/**1**/3.9/**1**/3.7/**1.2**/3.2/**1.2**/2.8/**1.2**/2.6/**1.2**/2.4/**1.2**/2.2/**1.2**/2.1/**1.3**/1.9/**1.4**/1.8/**1.5**/1.7/**1.6**/1.7 for sample M3255 and **2.3**/1.1/**1**/3.4/**1**/3.1/**1.2**/2.6/**1.2**/2.4/**1.2**/2.2/**1.2**/2/**1.2**/1.8/**1.2**/1.7/**1.3**/1.6/**1.4**/1.5/**1.5**/1.4/**1.6**/1.4 for M3253. The $AlAs_{0.56}Sb_{0.44}$ layers (barriers) are in bold font, the $In_{0.53}Ga_{0.47}As$ wells are in Roman font and the underlined layers are Si-doped to $n = 6\times10^{17}$ cm^{-3}.

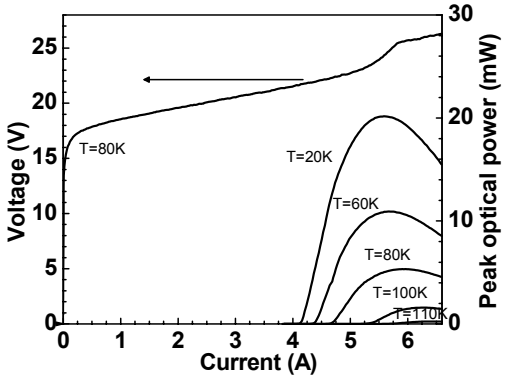

Fig. 3. Voltage-current (T = 80 K) and temperature dependent light-current characteristics for lattice matched InGaAs/AlAsSb QCL M3253 emitting at $\lambda \sim 3.05$ μm. The laser ridge is 20 μm wide and 1.5 mm long.

The realisation of QCLs in the $\lambda \sim 3$ μm region places particularly stringent demands on MBE growth, since the high QCL transition energy (~ 400 meV) requires the use of very thin (several monolayers) quantum well/barrier layers. For such structures, even very small fluctuations in layer thickness can cause variations in the positions of the higher energy electron levels of tens of meV, potentially leading to problems with inter-level misalignment under operating conditions. With this factor in mind, as well as the expected influence of X-valley on carrier dynamics and on reliability of the calculations for such high energies, it is unsurprising that the $\lambda \sim 3$ μm (M3253) laser exhibits reduced performance relative to longer wavelength devices. It is hard to estimate precisely by what extent the performance of this laser is affected by intervalley scattering and reduced accuracy for the calculations but we believe that the short wavelength design has considerable scope for optimisation.

2.3 Strain-compensated lasers

As the indium fraction in the InGaAs quantum wells increases, the energy separation between Γ-valley and the minima of X- and L-valleys also rises (Fig.4).[7] For the lattice matched $In_{0.53}Ga_{0.47}As$ composition the lowest satellite valley is at the X-point. For $In_{0.7}Ga_{0.3}As$ quantum wells, the L-valley becomes the lowest satellite valley and the energy difference between the minima of the Γ- and L-valleys is calculated (without taking into account the strain) to be about 620 meV. Thus for the strain compensated $In_{0.7}Ga_{0.3}As$/AlAsSb system the energy separation between upper laser level and the

minimum of the lowest satellite valley is estimated to increase by up to 80 meV relative to the lattice matched composition. Therefore QCLs based on the strain compensated InGaAs/AlAsSb material system potentially should be able to achieve emission wavelength as low as about 3.1 μm and the laser transitions in such devices are anticipated to be still free from the effects of intervalley scattering.

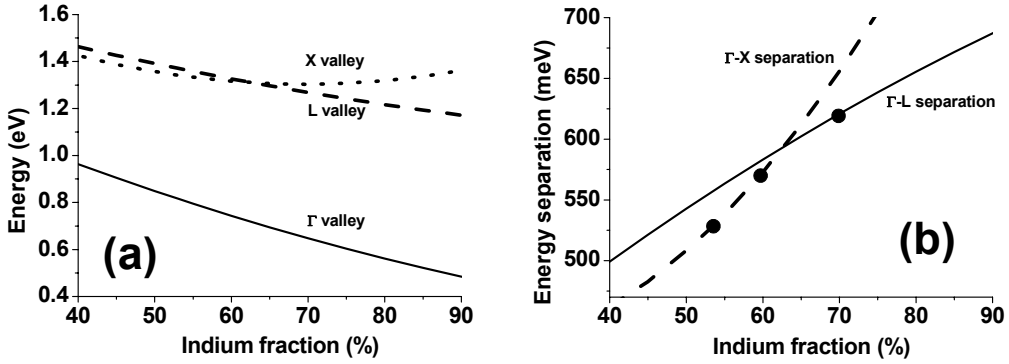

Fig. 4. The calculated positions (based on data presented in Ref. 7) of the minima for the conduction band valleys in InGaAs (a) and the energy separation between Γ-point and upper valleys (b) versus indium fraction.

Three QCL structures (M3254, M3257 and M3259) based on a design (for $\lambda = 4.1$ μm) with identical thicknesses of the quantum wells and barriers in the core regions were studied. The composition of the layers in the core regions of these devices is the only difference. The M3254 laser is a control sample based on the InP lattice matched $In_{0.53}Ga_{0.47}As/AlAs_{0.56}Sb_{0.44}$ system. The other two lasers are strain compensated. They have higher indium fraction in the InGaAs quantum wells: 60 and 70 % for M3259 and M3257 structures, respectively. The compressive strain induced by the InGaAs quantum wells was compensated by the tensile strain via increasing the As fraction and decreasing the Sb fraction in the AlAsSb barriers. The calculated conduction band profile under applied bias is shown in Fig.5 (a) for the $In_{0.7}Ga_{0.3}As$/AlAsSb M3257 laser. As indium fraction has been increased in the quantum wells, the electron effective mass for strain compensated structures becomes smaller and is calculated to be about $m^*=0.034$ for $In_{0.7}Ga_{0.3}As$ compared with $m^*=0.042$ for lattice matched $In_{0.53}Ga_{0.47}As$. Although smaller effective mass results in the energy positions of the electron levels in strain compensated InGaAs/AlAsSb quantum wells moving up, this energy shift is not very dramatic for the energy levels lying at several hundreds of meV above the bottom of the well, because of the strong influence of conduction band non-parabolicity at these high energies. The upper laser level for the M3257 device is calculated to increase in energy by about 10 meV relative to the upper laser level for the lattice matched M3254 device. The shift towards higher energies of the upper laser level for M3257 device, which is dependent on the expected increase of ΔE_c for the strained compensated compositions is estimated to add another 10 meV. The lower laser levels also increase in energy, giving a calculated overall increase in the laser transition energy of about 8 meV.

All three devices M3254, M3259 and M3257 display laser emission at temperatures up to at least 320 K (the limit of the cryostat used) and at wavelengths $\lambda \sim 4$ - 4.2 μm. These values, together with the effect of slightly decreased emission wavelength for the strained compensated lasers, are very close to those expected from the calculations. The lasers from different wafers show very similar performance (Fig.5 (b)) with average J_{th} equal to 3.4 kA/cm^2 at 80 K rising to 11 kA/cm^2 at 300 K. The characteristic temperature T_0 obtained in the range of 160 - 320 K is estimated to be between 140 and 175 K for different wafers and ridges. The pulsed optical peak power recorded for all three wafers is about 1 W at 80 K and about 150 mW at 300 K. A steady increase of emission power is observed with increasing current. The electroluminescence spectra obtained for all three wafers show very comparable full width at half maximum (FWHM) of the emission peaks for both 80 K (~ 40-45 meV) and 300 K (~ 65 – 70 meV) temperatures indicating that the quality of quantum well/barrier interfaces in strain compensated devices is as good as in the lattice matched M3254 laser.

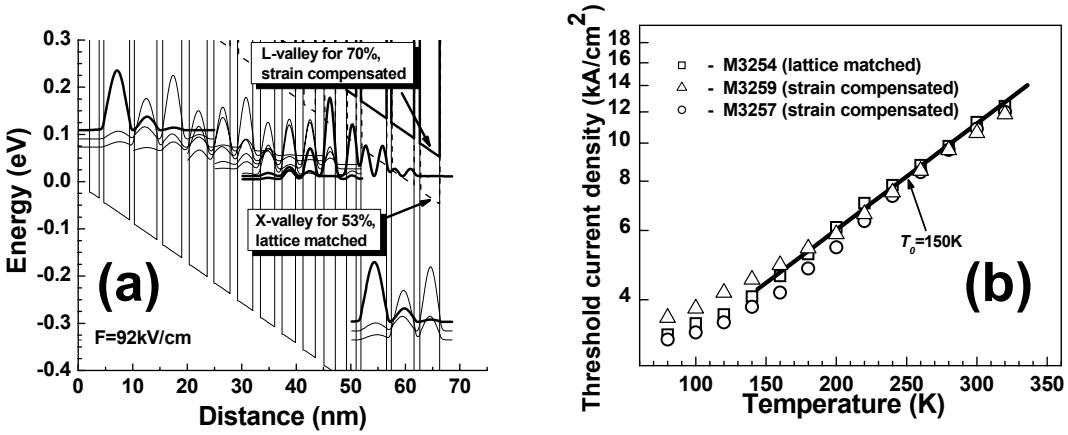

Fig. 5. Calculated conduction band profile (a) for strain compensated M3257 QCL and typical threshold current density dependence versus the heat sink temperature (b) for lattice matched M3254 and strain compensated QCLs. The layer thicknesses (in nanometers) starting from the injection barrier for one period of active and injector regions are as follows: **2.1**/1.8/**0.9**/4.6/**0.9**/4.2/**1.1**/3.5/**1.3**/3.3/**1.3**/3/**1.4**/2.7/**1.4**/2.6/**1.4**/2.4/**1.5**/2.2/**1.5**/2.1. The AlAsSb layers (barriers) are in bold font, the InGaAs wells are in Roman font and the underlined layers are Si-doped to n = 6×10^{17} cm^{-3}. The expected position of the lowest satellite valley (L-valley) minimum for M3257 laser is shown by thick lines. The expected position of the lowest satellite valley (X-valley) minimum for lattice matched M3254 laser is indicated by dashed lines.

2.4 Lasers with AlAs barriers

In order to verify the influence of AlAs layers on QCL performance AlAs barriers were introduced in the active region (where the intersubband laser transitions occur) of strain compensated $In_{0.6}Ga_{0.4}As/AlAs_{0.67}Sb_{0.33}$ QCLs. The $AlAs_{0.67}Sb_{0.33}$ barriers in the injector were left unmodified. The QCL structure (M3260) with the same design and layer compositions as for M3259 but with AlAs barriers in the active region was studied.

The calculated conduction band profile under applied bias is shown in Fig. 6 (a). Thin AlAs barriers are expected to introduce very small perturbation into these model calculations compared to the case of M3259 since AlAs has electron effective mass similar to AlAsSb. The expected lower conduction band offset (about 1.35 eV) for the $In_{0.6}Ga_{0.4}As/AlAs$ system should lead to slightly lower calculated energy of the laser transitions for wafer M3260 (290 meV compared to 300 meV for wafer M3259).

The observed operating characteristics of the M3260 lasers are significantly improved. These lasers display pulsed laser emission at wavelengths ($\lambda \sim 4.05$ μm) very close to the calculated values and demonstrate much better performance with average pulsed J_{th} equal to 1.4 kA/cm^2 at 80 K and 6.7 kA/cm^2 at 300 K (Fig. 6 (b)). The maximum pulsed optical peak power of about 500 mW recorded at 300 K and at 13 kA/cm^2 is also noticeably higher compared with lattice matched M3254 and strain compensated M3259 and M3257 lasers. However in contrast to the predictions made from the calculations the observed emission energy for the lasers from wafer M3260 is actually not lower but higher by 15 meV compared with the devices from wafer M3259. This wavelength shift can be explained if, for example, due to inter diffusion of the elements at InGaAs/AlAsSb interfaces the effective height of the $AlAs_{0.67}Sb_{0.33}$ barriers in the active region of the devices from wafer M3259 is actually somewhat lower than AlAs barriers in the lasers from wafer M3260. The current-voltage characteristics of the devices from wafer M3260 are practically identical to the strain compensated lasers M3257 and M3259, indicating that the introduction of AlAs barriers does not significantly affect injection efficiency into the active regions.

The electroluminescence spectra recorded for wafer M3260 for the current below laser threshold have narrower (by 10-15 meV) peaks compared with M3259 lasers. Reduced FWHM for the samples with AlAs barriers for both temperatures, 80 and 300 K, could be explained by the improved profile of the InGaAs wells due to suppressed inter diffusion at the InGaAs/AlAs interfaces, however, the exact mechanism of the electroluminescence peak broadening in InGaAs/AlAsSb QCLs is still to be investigated.

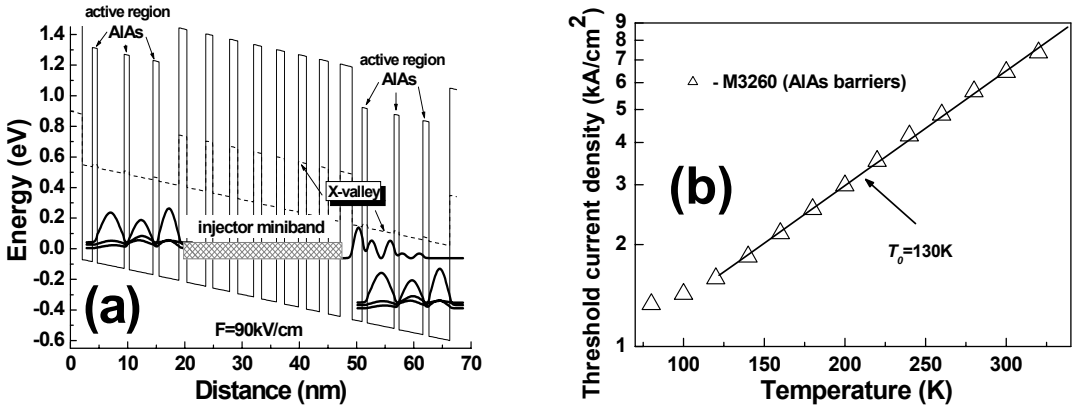

Fig. 6. Calculated conduction band profile (a) and typical threshold current density dependence versus the heat sink temperature (b) for the strain compensated $In_{0.6}Ga_{0.4}As/AlAs_{0.67}Sb_{0.33}$(AlAs) QCL (wafer M3260). The layer thicknesses (in nanometers) starting from the injection barrier for one period of active and injector regions are as follows: **2.1**/1.8/(**0.9**)/4.6/(**0.9**)/4.2/(**1.1**)/3.5/**1.3**/3.3/**1.3**/3/**1.4**/2.7/**1.4**/2.6/**1.4**/2.4/**1.5**/2.2/ **1.5**/2.1. The $AlAs_{0.67}Sb_{0.33}$ layers (barriers) are in bold font, the AlAs barriers are in bold font and in the parentheses, the $In_{0.6}Ga_{0.4}As$ wells are in Roman font and the underlined layers are Si-doped to $n = 6\times10^{17}$ cm^{-3}.

3. CONCLUSIONS

We have demonstrated room temperature pulsed operation of InP-based $In_{0.53}Ga_{0.47}As/AlAs_{0.56}Sb_{0.44}$ QCLs at wavelengths down to $\lambda \sim 3.57$ μm. Low temperature ($T <\sim 110$ K) operation of QCLs at much shorter wavelength ($\lambda \approx 3.05$ μm) has also been observed. The results show that the predicted onset of Γ-X intervalley scattering at QCL emission wavelengths of around 3.7 μm does not cause shut-down of laser action at shorter wavelengths in lattice matched $In_{0.53}Ga_{0.47}As/AlAs_{0.56}Sb_{0.44}$ structures.

We have proved the feasibility of strain compensated InP-based $In_xGa_{1-x}As$/AlAsSb QCLs. The lasers with x = 0.6 and 0.7 emit at room temperature in pulsed regime at wavelengths near 4.1 μm with laser performance very comparable with lattice matched $In_{0.53}Ga_{0.47}As/AlAs_{0.56}Sb_{0.44}$ QCLs with identical design. The realization of the strain compensated lasers without degradation in performance provides a basis for possible improvements in InGaAs/AlAsSb QCL designs for $\lambda <$ 3.5 μm, which are likely to benefit from the increased energy separation between Γ and satellite valleys provided by the strain compensated system.

We have presented the evidence that introduction of AlAs barriers in the active regions of strain compensated InP-based $In_{0.6}Ga_{0.4}As/AlAs_{0.67}Sb_{0.33}$ QCLs results in significant improvement in laser performance compared to the lasers with only $AlAs_{0.67}Sb_{0.33}$ barriers in the core region. The realization of the strain compensated InGaAs/AlAsSb lasers with AlAs barriers and higher fraction of indium in the quantum wells should have strong potential for further improving the performance of short wavelength InGaAs/AlAsSb QCLs.

ACKNOWLEDGEMENTS

This work is supported by the Department of Trade and Industry, UK, and by the European Union Marie Curie Research Training Network "POISE"

REFERENCES

[1] J. Devenson, R. Teissier, O. Cathabard, and A.N. Baranov, **"**InAs/AlSb quantum cascade lasers emitting below 3μm", Appl. Phys. Lett. **90**, 111118 (2007).

[2] J. Devenson, D. Barate, O. Cathabard, R. Teissier, and A.N. Baranov, "Very short wavelength (λ = 3.1 - 3.3 μm) quantum cascade lasers", Appl. Phys. Lett. **89**, 191115 (2006).

[3] J. Devenson, O. Cathabard, R. Teissier, and A.N. Baranov, "High temperature operation of λ ~ 3.3μm quantum cascade lasers", Appl. Phys. Lett. **91**, 141106 (2007).

[4] M.P. Semtsiv, M. Wienold, S. Dressler, and W.T. Masselink, "Short-wavelength (λ = 3.05 μm) InP-based strain-compensated quantum cascade laser", Appl. Phys. Lett. **90**, 051111 (2007).

[5] J.S. Yu, A. Evans, S. Slivken, S.R. Darvish, and M. Razeghi, "Temperature dependent characteristics of λ ~ 3.8 μm room-temperature continuous-wave quantum cascade lasers", Appl. Phys. Lett. **88**, 251118 (2006).

[6] Q. Yang, C. Manz, W. Bronner, K. Köhler, and J. Wagner, "Room-temperature short-wavelength (λ ~ 3.7-3.9 μm) GaInAs/AlAsSb quantum-cascade lasers", Appl. Phys. Lett. **88**, 121127 (2006).

[7] I. Vurgaftman, J.R. Meyer, and L.R. Ram-Mohan, "Band parameters for III-V compound semiconductors and their alloys" J. Appl. Phys. **89**, 5815 (2001).

[8] For example, T. Mozume and M. Georgiev, "Optical and structural characterization of InGaAs/AlAsSb quantum wells", Jpn. J. Appl. Phys. **41**, 1008-1011 (2002).

[9] A.V. Gopal, H. Yoshida, T. Simoyama, N. Georgiev, T. Mozume, and H. Ishikawa, "Well-width and doping-density dependence of 1.35μm intersubband transition in InGaAs/AlAsSb quantum wells", Appl. Phys. Lett. **80**, 4696 (2002).

[10] J. Faist, M. Beck, T. Aellen, and E. Gini, "Quantum-cascade lasers based on a bound-to-continuum transition", Appl. Phys. Lett. **78**, 147 (2001).

[11] D.G. Revin, L.R. Wilson, E.A. Zibik, R.P. Green, J.W. Cockburn, M. J. Steer, R. J. Airey, and M. Hopkinson, "InGaAs/AlAsSb quantum cascade lasers", Appl. Phys. Lett. **85**, 3992 (2004).